Spectrochimica Acta Part A: Molecular and Biomolecular Spectroscopy 255 (2021) 119734

Contents lists available at ScienceDirect

Spectrochimica Acta Part A: Molecular and Biomolecular Spectroscopy

journal homepage: www.elsevier.com/locate/saa

Upconversion nanoparticles-based FRET system for sensitive detection of *Staphylococcus aureus*

Qin Ouyang [a,*], Yongcun Yang [a], Shujat Ali [a,b], Li Wang [a], Huanhuan Li [a], Quansheng Chen [a,*]

[a] School of Food and Biological Engineering, Jiangsu University, Zhenjiang 212013, PR China
[b] College of Electrical and Electronic Engineering, Wenzhou University, Wenzhou 325035, PR China

HIGHLIGHTS

- A novel method for the determination of *S. aureus* was developed.
- Hexagonal-phase UCNPs were synthesized with good optical properties.
- A FRET-based aptarsensor was developed at range of 47–4.7 × 10^7 CFU/mL.
- Application in food samples of this aptarsensor has achieved good results.

GRAPHICAL ABSTRACT

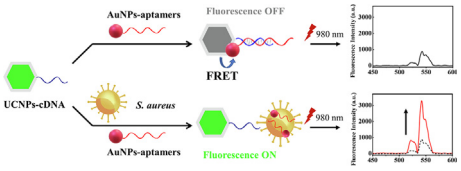

ARTICLE INFO

Article history:
Received 23 November 2020
Received in revised form 16 March 2021
Accepted 18 March 2021
Available online 23 March 2021

Keywords:
Staphylococcus aureus
Upconversion nanoparticles
Gold nanoparticles
Fluorescence resonance energy transfer
Aptamer

ABSTRACT

Staphylococcus aureus (*S. aureus*) is a pathogenic bacterium that seriously endangers food safety. Herein, a rapid, sensitive and specific aptasensor based on upconversion fluorescence resonance energy transfer (FRET) was developed for *S. aureus* detection in food. Aptamer-functionalized gold nanoparticles (AuNPs-aptamers) were bonded to cDNA-modified upconversion nanoparticles (UCNPs-cDNA) by complementary pairing, resulting in fluorescence quenching. After adding *S. aureus* into the system, the aptamers preferentially combined with *S. aureus*, dissociated UCNPs-cDNA from AuNPs-aptamers, and the fluorescence was recovered. Under optimized conditions, there was a significant linear correlation between fluorescence intensity and *S. aureus* concentration over the range 47–4.7 × 10^7 CFU/mL (R^2 = 0.9904) with a detection limit of 10.7 CFU/mL. Furthermore, the precision and accuracy of the developed biosensor were validated using standard plate count method, yielding no significant differences. The proposed method has potential application for rapid and sensitive quantification of *S. aureus* in food.

1. Introduction

Over the past few decades, outbreaks of food-borne diseases caused by the ingestion of foodstuffs contaminated with pathogenic bacteria have increased considerably [1]. *Staphylococcus aureus* (*S. aureus*) is a harmful foodborne pathogen that has received widespread attention in terms of food safety. High-protein foods, such as meat, fish, eggs, and milk, can be easily contaminated by *S. aureus* [2]. Generally, *S. aureus* causes minor skin infections, such as scalded skin syndrome, abscesses and carbuncles. However, certain infections can become life-threatening and deadly [3]. Hence, timely and specific detection of *S. aureus* in foods is essential to reduce the risk of human exposure to such bacteria and ensure food safety. Traditional methods for *S. aureus* detection include enrichment culture, colony counting, staining observations and coagulase tests, which take at least two days to achieve reliable results [4]. At present, several other methods such as loop-mediated isothermal amplification and real-time multiplex polymerase chain reaction have been applied for *S. aureus* detection. Despite the accuracy of these methods, they are more time-consuming and less cost-effective [5]. Hence, it is crucial to develop

* Corresponding authors.
E-mail addresses: oyqyf@ujs.edu.cn (Q. Ouyang), qschen@ujs.edu.cn (Q. Chen).

https://doi.org/10.1016/j.saa.2021.119734
1386-1425/

a rapid, simple, and sensitive approach for the detection of *S. aureus*.

To satisfy these demands, researchers have designed several aptasensors based on antibodies [6] or aptamers [7] as biological receptors for rapid and specific pathogen detection. In particular, fluorescence sensors with multiple advantages, such as ease of operation, rapid response, and high sensitivity, have received considerable interest from researchers. For example, Pebdeni et al. designed an ultrasensitive sensor based on carbon quantum dots for the detection of *S. aureus* in milk, orange juice and human serum [8]. Cui et al. established a fluorescence aptasensor for the separation and recognition of *S. aureus* using carbon dots [9]. Yi et al. described a fluorescence resonance energy transfer (FRET) probe based on 6-carboxyfluorescein for antibacterial susceptibility testing of *S. aureus* [10]. Although the above-mentioned approaches can offer accurate results, fluorescent dyes or quantum dots as signal reporters have a number of shortcomings in the analysis of actual samples, such as photobleaching, low water solubility, and background auto-fluorescence [11]. Alternatively, upconversion nanoparticles (UCNPs) have emerged as potential substitutes and offer substantial advantages over quantum dots and organic fluorophores [12]. UCNPs can emit visible luminescence under near-infrared (NIR) excitation owing to their unique anti-Stokes luminescence properties, which offer good chemical and optical stability, narrow emission spectra and no autofluorescence. To date, several antibody-based upconversion fluorescence sensors have been designed for *S. aureus* determination [13]. However, antibodies can be easily affected by temperature and pH, and thus require strict storage conditions [14]. Interestingly, aptamers (involving RNA or single-stranded DNA oligonucleotides) are emerging as promising candidates, that can bind to target molecules with high specificity and affinity by changing structural conformation [15]. Furthermore, it is much easier to synthesize, modify by chemical routes, and have good stability over a diverse range of pH, temperatures, and chemical and solvent concentrations [16].

Currently, detection of *S. aureus* has been performed by combining aptamers with magnetic separation in a UCNPs biosensor system [17]. However, the magnetic separation mode may have problems with the beads affecting the fluorescence intensity of the detection system, and potential sample loss in clean-up procedures [18]. Upconversion FRET biosensors are based on quencher particles as acceptors and UCNPs as donors, where nonradiative energy transfer occurs from donor to acceptor moieties via long-range dipole–dipole interactions [19]. There are two necessary criteria for the FRET process [20–22]. First, the emission spectrum of the donor and the absorption spectrum of the acceptor must overlap. Second, the distance between the donor and acceptor should be less than 10 nm. After fulfillment of the above two criteria, upconversion fluorescence has the possibility of quenching [23]. In a FRET system, the fluorescence can be quenched so as to enable target recognition by changes in fluorescence intensity. Hence, FRET does not require cleaning or sample separation steps. This wash-free strategy can simplify the assay procedure, reduce testing times, and minimizing experimental interference. Upconversion FRET aptasensors have been employed for the detection of biological samples such as circulating tumor DNA [24], *Escherichia coli* (*E. coli*) [25], and influenza H7N9 virus [26]. However, the detection of *S. aureus* has not yet been explored.

Herein, a novel FRET-based detection approach was developed for *S. aureus* using aptamer recognition with aptamer-functionalized gold nanoparticles (AuNPs) as the acceptor and UCNPs as the donor (Fig. 1). The AuNPs were functionalized with aptamers (specifically recognizing bacteria), whereas UCNPs were conjugated with aptamers of complementary DNA (cDNA). Owing to the complementary base pairing involving the cDNA and aptamers, the UCNPs interacted with the AuNPs and caused quenching of the upconversion fluorescence. AuNPs functionalized with aptamers preferentially bound to *S. aureus* (when added into the system) and released the UCNPs, resulting in the recovery of UCNPs fluorescence. Consequently, the system enabled the simple, sensitive and rapid detection of *S. aureus*.

2. Materials and methods

2.1. Materials and chemicals

Erbium (III) chloride hexahydrate ($ErCl_3{\cdot}6H_2O$, 99.9%), oleic acid (90%), yttrium (III) chloride hexahydrate ($YCl_3{\cdot}6H_2O$, 99.9%), 1-octadecene (90%) and ytterbium (III) chloride hexahydrate ($YbCl_3{\cdot}6H_2O$, 99.9%) were supplied by Sigma-Aldrich Company. Trisodium citrate dihydrate, chloroauric acid ($HAuCl_4$), polyacrylic acid (PAA, MW = 2000), tris (2-carboxyethyl) phosphine and sodium dodecyl sulfate (SDS) were obtained from Aladdin Reagent Co., Ltd. (Shanghai, China). Ethanol, methanol, chloroform, toluene, sodium chloride (NaCl, 99%), sodium hydroxide, ammonium fluoride, phosphate buffer saline (PBS, pH = 7.4), 1-ethyl-3-(3-dimethy laminopropyl)-carbodiimide hydrochloride (EDC), 2-(N-morpholino) ethane sulfonic acid (MES) (pH = 6), acetate buffer, and N-hydroxysulfosuccinimide sodium salt (sulfo-NHS) were purchased from Sinopharm Chemical Reagent Co., Ltd. (Shanghai, China). *E. coli* (ATCC 25922), *S. aureus* (ATCC 29213), *Bacillus subtilis* (*B. subtilis*) (ATCC 6633) and *Salmonella typhimurium* (*S. typhimurium*) (ATCC 50761) were got from the American Type Culture Collection (ATCC, Manassas, VA, USA). Sequences of aptamers and cDNA specific for *S. aureus* ATCC 29213 (Table S1) [27] were prepared by Sangon Biotechnology Ltd. (Shanghai, China). All chemicals without stated purity were analytical grade reagents and were used without further purification. A Milli-Q ultrapure water system supplied ultrapure water throughout the study (Millipore, USA).

2.2. Bacterial strains and culture conditions

In this study, *S. aureus* (ATCC 29213) was selected as the target bacteria for sensing, and *E. coli* (ATCC 25922), *S. typhimurium* (ATCC 50761) and *B. subtilis* (ATCC 6633) were selected as control groups. The selected bacterial strains were inoculated into 15 mL of Luria-Bertani medium at 37 °C for 12 h. After incubation, the bacteria were diluted 10-fold with PBS. One milliliter of each dilution was spread on plate count agar to obtain bacterial counts (CFU/mL).

2.3. Instrumentation

Upconversion luminescence (UCL) spectra were acquired using an RFS1000 fluorescence spectrometer (excitation wavelength 980 nm, optical path 1 cm, Oceanhood Opto-Eletronics Tech Ltd., China). The size and morphology of the UCNPs and AuNPs were determined using a JEOL 2100 transmission electron microscope (TEM) (JEOL, Ltd.). Fourier transform infrared (FT-IR) spectra of the UCNPs were collected using a Nicolet Nexus 470 Fourier transform infrared spectrophotometer (Thermo Electron Co., USA) based on the potassium bromide pellet pressing method. The crystallinity of the UCNPs was determined using X-ray diffraction (XRD, Rigaku 2500). The 2θ angles of the XRD spectra were acquired at a scanning rate of 5°/min. A Malvern Zetasizer Nano ZS90 (Malvern Instruments Ltd., UK) was employed for zeta potential analysis. UV–Vis absorption spectra of AuNPs and aptamers were measured using a UV-2450 spectrophotometer (Shimadzu, Japan) after baseline calibration using PBS.

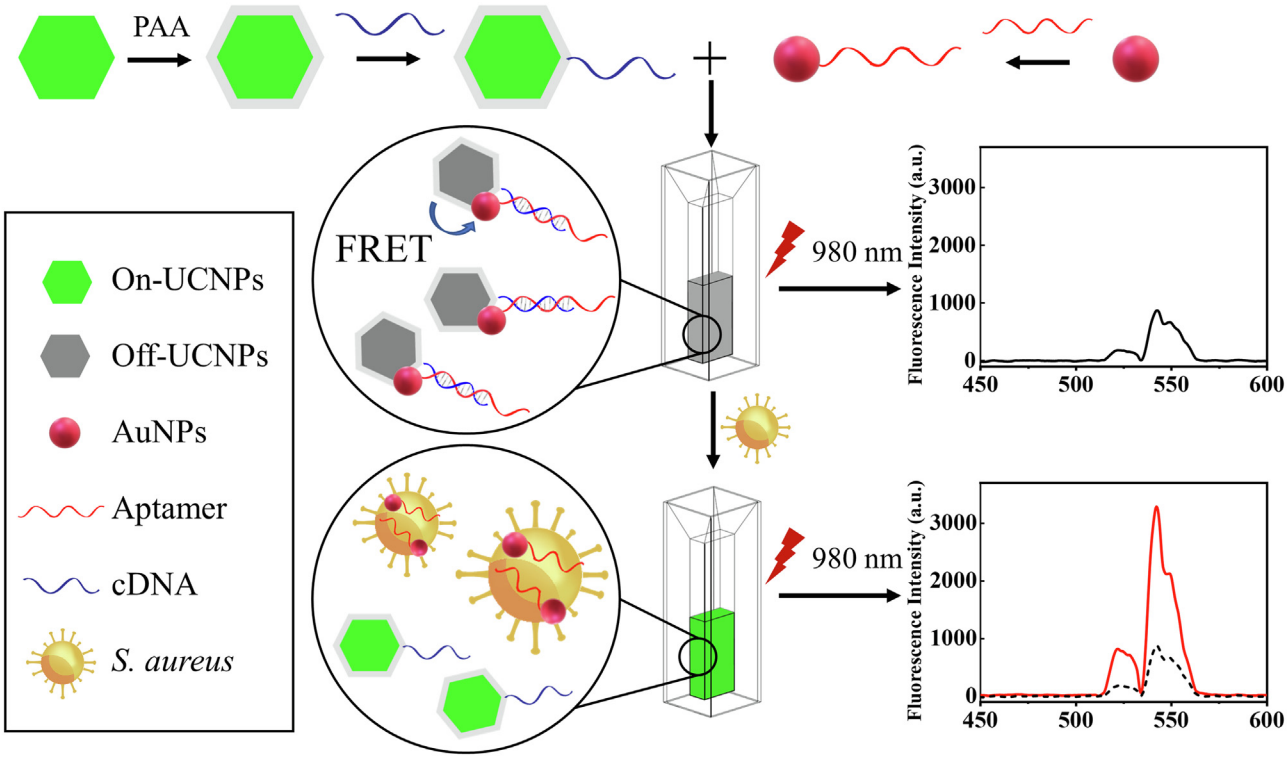

Fig. 1. Schematic principle of the designed aptasensor for *S. aureus* detection.

2.4. Synthesis and modification of UCNPs

The $NaYF_4$: Yb, Er UCNPs were synthesized using a previously reported thermal decomposition procedure with minor modifications [28]. In detail, 0.18 mmol $YbCl_3$, 0.8 mmol YCl_3 and 0.02 mmol $ErCl_3$ were dissolved in 10 mL methanol. The obtained solution was mixed with 1-octadecene (17.5 mL) and oleic acid (7.5 mL) in a 150 mL round-bottom flask. To remove oxygen, argon was introduced into the system for 15 min and the obtained solution was stirred at 160 °C for 50 min. After the reaction mixture was cooled to 45 °C, 15 mL methanol of ammonium fluoride (0.1482 g) and sodium hydroxide (0.1 g) were added dropwise. Then, the reaction mixture was stirred at 45 °C for 30 min, followed by further heating at 75 °C for 30 min under an argon atmosphere to entirely eliminate methanol and air. Finally, the reaction mixture was heated to 290 °C for 2 h to form nanocrystals. The final product was centrifuged and washed three times with absolute ethanol and methanol. After drying at 40 °C, the white UCNPs were collected.

To acquire hydrophilic UCNPs, PAA was used to replace hydrophobic oleic acid (OA) via a ligand-exchange procedure [29]. OA-$NaYF_4$: Yb UCNPs (50 mg) were dispersed in 10 mL of a solution of chloroform and toluene (v/v = 2:3). Next, the solution was added to 15 mL of an aqueous solution of PAA (400 mg) and stirred for 24 h. The modified nanomaterials were obtained by centrifugation at 10,000 rpm for 5 min and then washed three times with ethanol and water to remove excess reagents. The obtained water-soluble PAA-capped UCNPs were resuspended in 10 mL of water.

2.5. Attachment of amino cDNA to UCNPs-PAA

MES buffer (1 mL, 50 mM, pH = 6) was added to a 1 mL solution of carboxyl-modified UCNPs-PAA. Sulfo-NHS (1 mg) and EDC (0.5 mg) were added to initiate carboxyl activation on the surface of the UCNPs. Then, the UCNPs were centrifuged at 6,000 rpm and washed twice with PBS buffer solution (pH = 7.4). Then, the UCNPs were resuspended in 2 mL of PBS buffer solution and 1.2 mL of 1 μM amino-modified cDNA was subsequently added. The mixture was incubated in a rotary mixer for 2 h at 37 °C. After washing with ultrapure water, cDNA-modified UCNPs (UCNPs-cDNA) were resuspended in 2 mL STE buffer (pH = 8, 10 mM Tris-HCl, 1 mM EDTA and 100 mM NaCl) and stored at 4 °C.

2.6. Synthesis of aptamer-functionalized gold nanoparticles

AuNPs were synthesized according to a previously described method with certain modifications [30]. First, 50 mL of $HAuCl_4$ solution (1 mmol/L) was added to a 100 mL round-bottom flask and heated to boiling for 5 min with magnetic stirring. Then, 10 mL trisodium citrate (38.8 mmol/L) was rapidly injected and reacted for another 30 min. The yellow solution immediately turned blue and then remained wine-red. Finally, AuNPs were obtained and stored at 4 °C.

To activate thiolated oligonucleotide aptamers, 2 μL of tris (2-carboxyethyl) phosphine (10 mM), 10 μL of acetate buffer, (500 mM, pH = 4.8) and ultrapure water were mixed with aptamers, and incubated at 25 °C for 1 h. 1 mL AuNPs solution was added to the activated aptamers and shaken at 25 °C for 16 h. Next, SDS and NaCl were added to the above solution to obtain 0.16 M NaCl and 0.01% SDS solution. After shaking for 24 h, the reaction mixture was centrifuged at 12,000 rpm for 30 min and washed three times with ultrapure water. Finally, aptamer-functionalized AuNPs (Apt-AuNPs) were obtained, redispersed in STE buffer and stored at 4 °C.

2.7. Construction of aptasensor and detection of S. Aureus

First, reaction conditions and concentrations were optimized. In detail, 0.1 mg/mL cDNA-UCNPs were incubated with a series of concentrations of Apt-AuNPs at 37 °C for 120 min and upconver-

sion fluorescence spectra were recorded every 10 min. The concentration of Apt-AuNPs that resulted in the highest fluorescence quenching was taken as the optimal concentration, and the time when the fluorescence was stable were selected as the best reaction time. During the typical FRET detection process, various concentrations of known bacterial standards were added to the constructed aptasensor and the upconversion fluorescence spectra were examined.

2.8. Recovery experiments for sample

Fresh pork and beef meat samples were purchased from a local supermarket in Zhenjiang, China. To eliminate interference by *S. aureus* or other potential pathogenic bacteria, 25 g fresh meat was washed with sterile saline and exposed to a 30 W UV lamp for 15 min in a biosafety cabinet. Then, 1 mL of *S. aureus* at concentrations of 1×10^5, 1×10^6 and 1×10^7 CFU/mL were added to the meat samples and incubated for 10 min. The *S. aureus*-spiked meat samples were transferred to a flask containing 100 mL sterile saline and homogenized for 3 min. Finally, the prepared samples were assayed three times by the traditional plate counting method and the proposed method proposed here.

3. Results and discussion

3.1. Characterization of AuNPs and UCNPs

We conducted a series of characterizations, including TEM, FT-IR, XRD, UV–Vis spectra, and fluorescence spectra, to evaluate the crystallinity, surface modification, and morphology of UCNPs. The EDS spectra (Fig. S1) showed that the synthesized UCNPs were mainly composed of fluorine, sodium, yttrium, ytterbium and erbium elements. The UCNPs were prepared using Yb^{3+} as an sensitizer, Er^{3+} as activator and $NaYF_4$ as the host material. TEM imagines (Fig. 2A) showed that the $NaYF_4$:Yb, Er UCNPs were hexagonal and monodispersed particles with an average diameter of 20 nm. TEM results (Fig. 2B) for the AuNPs indicated that the AuNPs were uniformly dispersed with a particle size of approximately 14 nm. XRD patterns (Fig. 2C) showed that all of the diffraction peaks of synthesized UCNPs corresponded to the hexagonal structure of $NaYF_4$ (JCPDS no. 16–0334), illustrating that the UCNPs were purely hexagonal. The upconversion efficiency of hexagonal-phase UCNPs can be approximately ten-times that of its cubic phase counterparts [31]. The fluorescence spectra of UCNPs (Fig. 3D) exhibited four emission peaks centered at 658, 543, 524, and 409 nm when excited by 980 nm illumination. These could be assigned to the $^4F_{9/2} \rightarrow {}^4I_{15/2}$, $^4S_{3/2} \rightarrow {}^4I_{15/2}$, $^2H_{11/2} \rightarrow {}^4I_{15/2}$ and $^2H_{9/2} \rightarrow {}^4I_{15/2}$ transitions of Er^{3+}, respectively (Fig. 3E) [32]. To enhance the dispersibility of UCNPs in water, PAA was fabricated on the surface of the UCNPs. PAA substituted the oleic acid ligands from the surface of the UCNPs, and the carboxyl group of PAA was bound to the aptamer molecules. The presence of PAA molecules was confirmed by FT-IR spectroscopy (Fig. 2D). Before ligand exchange (Fig. 2D (b)), the spectrum of bare UCNPs exhibited a unique band at 2928 cm^{-1}, which was assigned to the asymmetric stretching vibration of the methylene group (-CH_2-), while its symmetric stretching vibration was noted at 2854 cm^{-1}. The peak at 3008 cm^{-1} is associated with the asymmetric stretching vibration of methyl (-CH_3) in the oleic acid ligand. The two peaks at 1558 and 1457 cm^{-1} were ascribed to the symmetric and asymmetric stretching vibrations of the carboxylic group (-COO-) of oleic acid. After the ligand exchange (Fig. 2D (a)), the band at 2945 cm^{-1} attributed to the asymmetric stretching of the -CH_2- group became inconspicuous while the broad band at 3425 cm^{-1} related to the stretching vibration of the -OH group became stronger. Meanwhile, the bands at 1715 and 1561 cm^{-1} indicated an increase in the number of -COOH groups. As shown in Fig. 2E, the zeta potential values of the AuNPs-aptamers and UCNPs-cDNA were negative. It further confirmed that the successful conjugation of AuNPs-aptamers and UCNPs-cDNA was due to the complementary base pairing of cDNA and aptamers rather than electrostatic adsorption.

UV–Vis spectra were measured to confirm the successful conjugation of carboxyl-functionalized UCNPs to cDNA, and of the AuNPs to thiol-modified aptamers. There was no absorption peak for bare AuNPs and UCNPs (Fig. 3A and B, black solid line). After binding with the aptamer and cDNA, an absorption peak at 260 nm was observed (Fig. 3A and B, red solid line). These results confirmed that the UCNPs and AuNPs were successfully conjugated to the cDNA and aptamers, respectively [33]. Furthermore, as shown in the inset of Fig. 3B, the absorption peak of the AuNPs aptamer conjugates revealed a 6 nm red shift (from 520 to 526 nm, with normalized absorbance), which could be related to the conjugation of AuNPs and aptamers [34].

3.2. Aptasensor-based detection of S. Aureus

Our strategy for *S. aureus* detection was established on the FRET-based aptasensor, as schematically described in Fig. 1. The efficiency of FRET depends on the overlap region between the emission spectra of the donor and the absorption spectra of the acceptor and the maintenance of an optimum distance separating the donor and acceptor molecules. UCNPs absorption, UCNPs fluorescence, AuNPs absorption, and AuNPs fluorescence spectra with normalized absorbance and fluorescence are presented in Fig. S3. The AuNPs showed a strong absorption band at 520 nm (Fig. S3 red dotted line), and UCNPs presented a fluorescence emission peak at 543 nm (Fig. S3, black solid lines). The AuNPs absorption band overlapped with the UCNPs fluorescence emission peak (543 nm). The UCNPs were conjugated with cDNA (Fig. 3A), while the AuNPs were functionalized with *S. aureus* aptamers (Fig. 3B). The distance between AuNPs and UCNPs was shortened by complementary base pairing of cDNA and aptamers.

Additionally, the influence of AuNPs concentration of on FRET efficiency was investigated. As shown in Fig. S5B, a gradual decrease in fluorescence intensity at 543 nm was observed with the increased concentration of AuNPs. The data were analyzed using the Stern–Volmer equation [35]. The relationship between I_0/I and [Q] is shown in Fig. S5A. Thus, the quenching constant was estimated to be 0.1661×10^9 M^{-1}.

$$\frac{I_0}{I} = 0.1661 \times [Q] + 1 (R^2 = 0.9906) \quad (1)$$

where I_0 and I are the fluorescent intensities of UCNPs in the absence and presence of AuNPs, respectively, and where [Q] is the concentration of AuNPs in nM.

The energy transfer efficiency (E) can be obtained from [36].

$$E = 1 - \frac{F}{F_0} = \frac{R_0^6}{R_0^6 + r^6} \quad (2)$$

where F and F_0 are the emission intensities of the donor in the presence and absence of the acceptor, respectively, r is the distance between the donor and acceptor, and R_0 is the critical distance at which the extent of energy transfer is 50%. R_0 can be calculated using the following equation [36].

$$R_0 = 0.0211 \left(J \Phi k^2 n^{-4} \right)^{1/6} \quad (3)$$

where k^2 is the spatial factor of orientation, n is the refractive index of the medium, Φ is the fluorescence quantum yield of the donor,

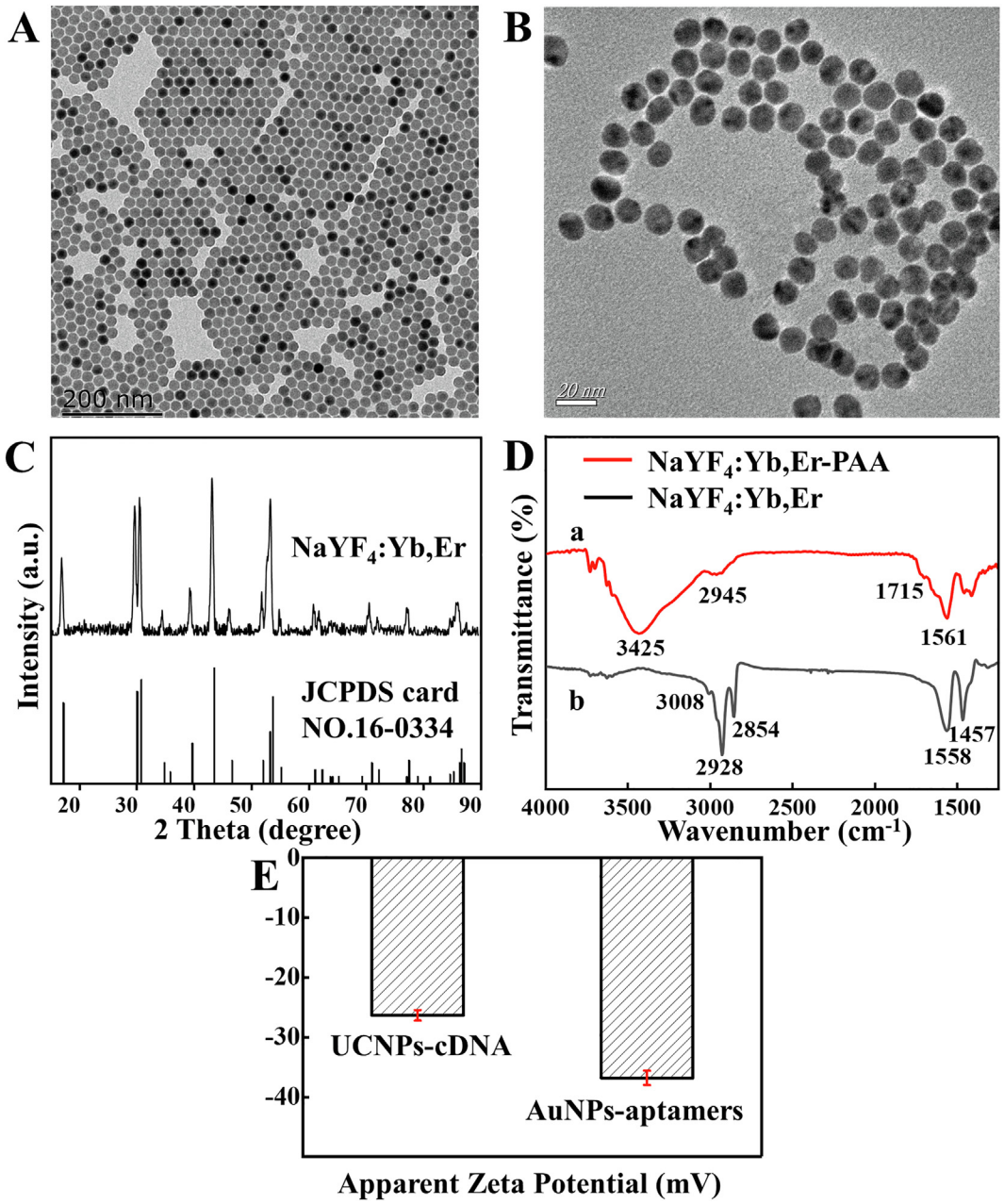

Fig. 2. (A) TEM image of NaY0.8F4:Yb0.18, Er0.02 (UCNPs); (B) TEM image of AuNPs; (C) XRD patterns of UCNPs; (D) FT-IR spectroscopy of UCNPs (black line) and UCNPs-PAA (red line); (E) ζ-potential of UCNPs-cDNA and AuNPs-aptamers.

and J is the overlap integral between donor emission and acceptor absorption, and is defined as [36]:

$$J(\lambda) = \int_0^\infty F(\lambda)\varepsilon(\lambda)\lambda^4 d\lambda \quad (4)$$

where $F(\lambda)$ is the fluorescence of the donor over the wavelength range λ to λ + dλ, and ε(λ) is the molar extinction coefficient of the acceptor at wavelength λ. The quantification of overlap can be expressed as J (normalized spectral overlap integral; units M^{-1}-$cm^{-1}nm^4$). Using the calculated value of J = 14.94 $M^{-1}cm^{-1}nm^4$ and the values for $k^2 = 2/3$, n = 1.335 and Φ = 0.24, the R_0 and r values were found to be 4.34 nm and 3.44 nm, respectively.

Such FRET measurements thus supported the fact that the probe is in very close proximity to the UCNPs-cDNA with tight binding characteristics. The FRET aptasensor was established involving AuNPs-aptamers and UCNPs-cDNA, resulting in fluorescence quenching (Fig. 3C, black dotted line). After *S. aureus* was added, aptamers specifically bound to *S. aureus*, resulting in the separation of AuNPs-aptamers and UCNPs-cDNA. FRET was inhibited by increasing distance, and upconversion fluorescence was recovered. This evidence could explain the occurrence of FRET. The value of the upconversion fluorescence recovery was proportional to the *S. aureus* concentration.

3.3. Optimization of detection parameters

It is necessary to optimize the parameters that can influence the accuracy of detection results. AuNPs-aptamers concentration can affect the detection system. When an excess of AuNPs-aptamers was added to the detection system, the free AuNPs-aptamers (not bound to UCNPs-cDNA) were bound to *S. aureus* without changing the fluorescence spectra, thus affecting the detection

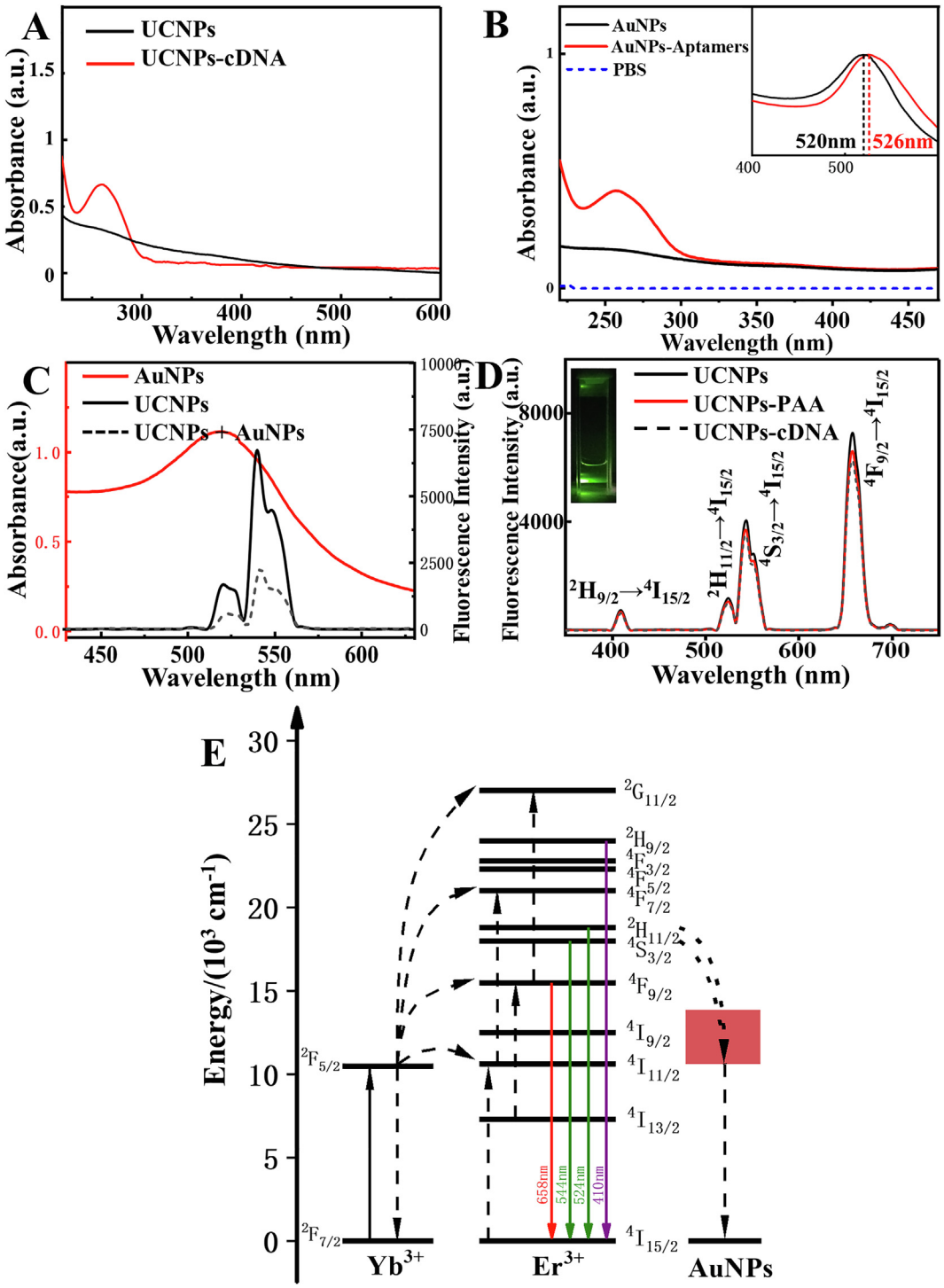

Fig. 3. (A) UV–Vis spectra of UCNPs before and after attachment of cDNA; (B) UV–Vis spectra of AuNPs before and after aptamer modification; inset shows that the absorption peak of AuNPs experienced a minor red-shift; (C) UV–vis absorption spectrum of AuNPs (red solid line), upconversion fluorescence emission spectrum of UCNPs (black solid line) and fluorescence spectrum of the solution after mixing UCNPs and AuNPs (black dotted line); (D) Fluorescence spectrum of UCNPs, UCNPs-PAA and UCNPs-cDNA, inset shows photograph of UCNPs-PAA excited by 980 nm laser illumination; (E) The energy transfer process of the constructed aptasensor.

limit. However, at low concentrations of AuNPs aptamer, the concentration of the FRET aptasensor was insufficient to react with the target bacteria, thereby reducing the upper limit of detection. Hence, varying volumes (0–250 μL) of the AuNPs-aptamers were added to 1 mL of the detection system with a fixed concentration (100 μL) of UCNPs-cDNA (1 mg/mL) to optimize the dosages of AuNPs-aptamers. Fig. 4A shows that the fluorescence intensity of UCNPs at 543 nm was constantly reduced with increasing AuNPs-aptamers concentrations, and maximum quenching efficiency was obtained at 150 μL. Consequently, the optimal concentration of AuNPs-aptamers was 150 μL in subsequent experiments. As presented in Fig. 4B, the upconversion fluorescence intensity steadily decreased with increasing elapsed time, and reached equilibrium at 0.5 h. Therefore, 0.5 h was adopted as the optimum reaction time in subsequent experiments. Finally, we optimized the effect of pH on fluorescence quenching efficiency and the

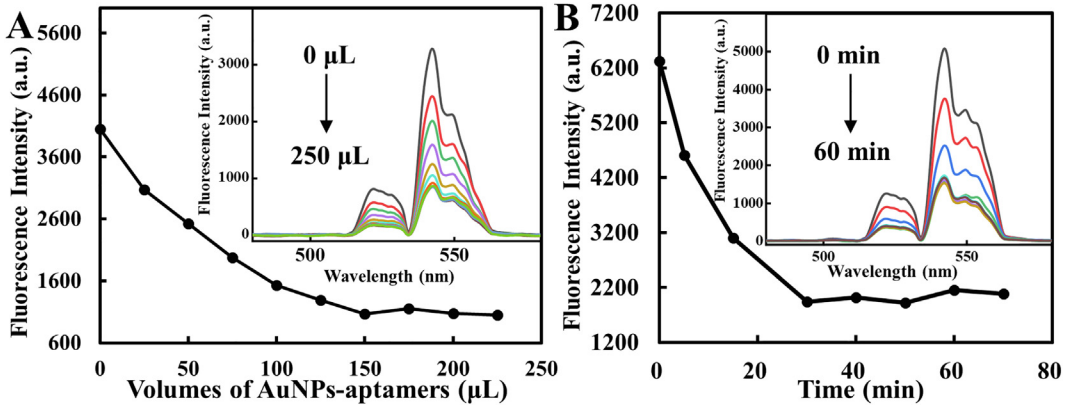

Fig. 4. Optimization experiments surrounding volumes (A) AuNPs and (B) incubation times.

maximum fluorescence quenching efficiency was obtained at pH = 7.4 (Fig. S4).

3.4. Determination of S. aureus

When *S. aureus* was introduced to the detection system, AuNPs-aptamers specifically bound to target bacteria. Consequently, FRET inhibition resulted in the recovery of UCNPs fluorescence. As shown in Fig. 5, when the concentration of *S. aureus* increased, the upconversion fluorescence intensity at 543 nm progressively recovered. The linear diagram indicates that the fluorescence intensity at 543 nm had a linear relationship with the logarithm of *S. aureus* concentration over the detection range of 47–4.7 × 10^7 CFU/mL and the linear equation was y = 209x + 1402 (R^2 = 0.9904). where x is the concentration of *S. aureus*, and y is the fluorescence intensity at 543 nm. The detection limit of *S. aureus* was 10.7 CFU/mL, as calculated using the formula: LOD = $3S_0/S$, where S is the slope of the standard curve and S_0 is the standard deviation of blank samples (n = 3). In addition, the obtained linear range and LOD were compared with other reported methods for *S. aureus* detection (Table S2). Considering the detection range, detection limit and simplicity of the experimental operation, the proposed method showed certain advantages and could be used for the quantitative detection of foodborne pathogens.

3.5. Specificity of FRET-based aptasensor

To assess the specificity of the proposed aptasensor for *S. aureus* (ATCC 29213) detection, 1 × 10^5 CFU/mL of other bacteria, *S. typhimurium*, *E. coli*, and *B. subtilis*, were added to the samples. As shown in Fig. S2, only *S. aureus* induced significant fluorescence recovery at 543 nm, and the fluorescence signals did not increase even with higher concentrations of the other pathogenic bacteria. These results indicated that the FRET-based aptasensor exhibited excellent specificity for *S. aureus* in the presence of non-target microorganisms. The high specificity of the aptasensor might be attributed to the design of UCNPs-cDNA-aptamer-AuNPs conjugates, in which the aptamer specifically identifies binding targets on the surface of *S. aureus*.

3.6. Determination of S. aureus in spiked matrices

The authenticity of the developed aptasensor for food sample analysis was validated by the detection of spiked samples. After sterilization treatment, several different concentrations of *S. aureus* were spiked into meat samples for subsequent detection. Table 1 shows the results of recovery experiment. The recovery of pork and beef samples was in the range of 99–103% and 91–97%, respectively. Their relative standard deviation (RSD) values ranged from 4.04 to 7.50% with three repetitions. Meanwhile, the results of proposed method were compared with those of the traditional plate count method, and the data of the two methods showed no statistically significant difference (P > 0.05). Such satisfactory results indicated that the designed aptasensor can capably detect *S. aureus* in food samples.

3.7. Storage stability and regeneration test of the developed aptasensor

The detection performance of the developed aptasensor storage for 3, 5, and 10 days was studied. As shown in Fig. S6, on day 10,

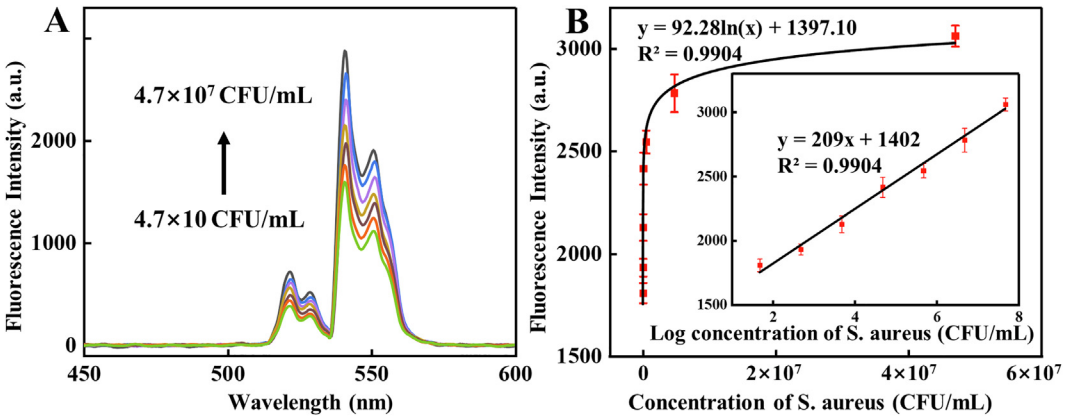

Fig. 5. Detection of *S. aureus* at different concentrations; (A) Fluorescence spectra of *S. aureus* at different concentrations; (B) Standard curve of fluorescence intensity at 543 nm vs. *S. aureus* concentration.

Table 1
Detection of *S. aureus* in real samples of this method and the plate counting method.

Samples	Adulterated concentration (CFU/mL)	Plate counting method			The developed method			P[c]
		Found ± SD[a] (CFU/mL)	Recovery (%)	RSD[b] (%)	Found ± SD[a] (CFU/mL)	Recovery (%)	RSD[b] (%)	
Pork	1.0×10^3	$(0.95 \pm 0.07) \times 10^3$	95	7.37	$(0.99 \pm 0.04) \times 10^3$	99	4.04	0.12
	1.0×10^4	$(0.98 \pm 0.08) \times 10^4$	98	8.10	$(1.03 \pm 0.07) \times 10^4$	103	6.80	
	1.0×10^5	$(0.98 \pm 0.09) \times 10^5$	98	8.71	$(0.99 \pm 0.04) \times 10^5$	99	4.04	
Beef	1.0×10^3	$(0.95 \pm 0.07) \times 10^3$	95	7.59	$(0.97 \pm 0.06) \times 10^3$	97	7.07	0.58
	1.0×10^4	$(0.93 \pm 0.08) \times 10^4$	93	8.66	$(0.95 \pm 0.07) \times 10^4$	95	7.50	
	1.0×10^5	$(0.92 \pm 0.07) \times 10^5$	92	7.43	$(0.91 \pm 0.09) \times 10^5$	91	3.90	

[a] SD: standard deviation, n = 3.
[b] RSD: relative standard deviation.
[c] P: P > 0.05 indicating no significant difference.

the upconversion fluorescence could still be quenched by AuNPs, and the detection of *S. aureus* could be effectively realized. Therefore, the aptamer sensor exhibited good stability. In order to conduct regeneration test, two groups of aptasensors synthesized at different times were used to detect *S. aureus* (1×10^4 CFU/mL). As shown in Table S3, there was no significant difference between the detection results for the two groups by *t*-test (P > 0.05), which indicated that the developed aptasensor had good reproducibility.

4. Conclusion

A FRET-based aptasensor was successfully designed for sensitive, specific and rapid detection of *S. aureus* in genuine food samples. By exploiting the high fluorescence quenching effect of the AuNPs and the aptamer target specificity, the amount of *S. aureus* was quantitatively detected over a linear range of 47–4.7×10^7 CFU/mL, and the assay exhibited an LOD of 10.7 CFU/mL. In addition, the developed aptasensor was successfully applied to sense *S. aureus* spiked into pork and beef samples, and exhibited satisfactory recovery percentages. The results of the proposed method were consistent with those of the national standard method. Therefore, the proposed aptasensor has promising potential for the detection of pathogenic bacteria in food samples.

CRediT authorship contribution statement

Qin Ouyang: Conceptualization, Investigation, Resources, Writing - original draft, Writing - review & editing, Project administration, Funding acquisition. **Yongcun Yang:** Conceptualization, Methodology, Software, Formal analysis, Writing - original draft. **Shujat Ali:** Writing - review & editing. **Li Wang:** Investigation. **Huanhuan Li:** Formal analysis, Investigation. **Quansheng Chen:** Supervision.

Declaration of Competing Interest

The authors declare that they have no known competing financial interests or personal relationships that could have appeared to influence the work reported in this paper.

Acknowledgments

This work has been financially supported by National Key Research and Development Program of China (2017YFC1600801), Natural Science Foundation of Jiangsu Province (BK20190100), and Project of Faculty of Agricultural Equipment of Jiangsu University.

Appendix A. Supplementary material

Supplementary data to this article can be found online at https://doi.org/10.1016/j.saa.2021.119734.

References

[1] M. Rubab, H.M. Shahbaz, A.N. Olaimat, D.-H. Oh, Biosensors for rapid and sensitive detection of Staphylococcus aureus in food, Biosens. Bioelectron 105 (2018) 49–57.
[2] J.H. Yoon, S. Wei, D.H. Oh, A highly selective enrichment broth combined with real-time PCR for detection of Staphylococcus aureus in food samples, LWT-Food Sci. Technol. 94 (2018) 103–110.
[3] M. Shahdordizadeh, S.M. Taghdisi, N. Ansari, F. Alebooye Langroodi, K. Abnous, M. Ramezani, Aptamer based biosensors for detection of Staphylococcus aureus, Sens. Actuator B-Chem 241 (2017) 619–635.
[4] M.Y. Wang, H.L. Yang, Y. Wu, Z.F. Fu, Fluorescent analysis of Staphylococcus aureus by using daptomycin and immunoglobulin G for dual sites affinity, Spectrochim, Acta Part A Mol. Biomol. Spectrosc 215 (2019) 340–344.
[5] U. Farooq, M.W. Ullah, Q. Yang, A. Aziz, J. Xu, L. Zhou, S. Wang, High-density phage particles immobilization in surface-modified bacterial cellulose for ultra-sensitive and selective electrochemical detection of Staphylococcus aureus, Biosens. Bioelectron 157 (2020) 112163.
[6] H.S. Wang, Y. Xiu, Y. Chen, L.P. Sun, L.B. Yang, H.H. Chen, X.D. Niu, Electrochemical immunosensor based on an antibody-hierarchical mesoporous SiO_2 for the detection of Staphylococcus aureus, RSC Adv. 9 (2019) 16278–16287.
[7] X.H. Shi, J.L. Zhang, F.J. He, A new aptamer/polyadenylated DNA interdigitated gold electrode piezoelectric sensor for rapid detection of Pseudomonas aeruginosa, Biosens. Bioelectron 132 (2019) 224–229.
[8] A.B. Pebdeni, M. Hosseini, M.R. Ganjali, Fluorescent turn-on aptasensor of Staphylococcus aureus based on the FRET between green carbon quantum dot and gold nanoparticle, Food Anal. Meth. 13 (2020) 2070–2079.
[9] F.C. Cui, J.D. Sun, J.D. Habimana, X.X. Yang, J. Ji, Y.Z. Zhang, H.T. Lei, Z.J. Li, J.Y. Zheng, M.H. Fan, X.L. Sun, Ultrasensitive fluorometric angling determination of staphylococcus aureus in vitro and fluorescence imaging in vivo using carbon dots with full-color emission, Anal. Chem 91 (2019) 14681–14690.
[10] S.Y. Yi, J. Jeong, K.E. Kim, K. Park, Y.B. Shin, Staphylococcus aureus specific FRET probe-based antibacterial susceptibility testing (SF-AST) by detection of micrococcal nuclease activity, ACS Infect. Dis. 6 (2020) 215–223.
[11] R.M. Renuka, N. Maroli, J. Achuth, K. Ponmalai, K. Kadirvelu, Highly adaptable and sensitive FRET-based aptamer assay for the detection of Salmonella paratyphi A, Spectrochim Acta Part A Mol. Biomol. Spectrosc 243 (2020).
[12] Q. Chen, R. Sheng, P. Wang, Q. Ouyang, A. Wang, S. Ali, M. Zareef, M.M. Hassan, Ultra-sensitive detection of malathion residues using FRET-based upconversion fluorescence sensor in food, Spectrochim Acta Part A Mol. Biomol. Spectrosc 241 (2020).
[13] B. Zhang, H. Li, W. Pan, Q. Chen, Q. Ouyang, J. Zhao, Dual-color upconversion nanoparticles (UCNPs)-based fluorescent immunoassay probes for sensitive sensing foodborne pathogens, Food Anal. Meth. 10 (2017) 2036–2045.
[14] S. Dai, S. Wu, N. Duan, J. Chen, Z. Zheng, Z. Wang, An ultrasensitive aptasensor for Ochratoxin A using hexagonal core/shell upconversion nanoparticles as luminophores, Biosens. Bioelectron 91 (2017) 538–544.
[15] X. Guo, F. Wen, N. Zheng, M. Saive, M.-L. Fauconnier, J. Wang, Aptamer-based biosensor for detection of mycotoxins, Front. Chem. 8 (2020).
[16] S. Ramlal, B. Mondal, P.S. Lavu, B. N, J. Kingston, Capture and detection of Staphylococcus aureus with dual labeled aptamers to cell surface components, Int. J. Food Microbiol. 265 (2018) 74–83.
[17] H. Li, W. Ahmad, Y. Rong, Q. Chen, M. Zuo, Q. Ouyang, Z. Guo, Designing an aptamer based magnetic and upconversion nanoparticles conjugated fluorescence sensor for screening Escherichia coli in food, Food Control 107 (2020) 106761.
[18] B. Jin, S. Wang, M. Lin, Y. Jin, S. Zhang, X. Cui, Y. Gong, A. Li, F. Xu, T.J. Lu, Upconversion nanoparticles based FRET aptasensor for rapid and ultrasenstive bacteria detection, Biosens. Bioelectron 90 (2017) 525–533.

[19] R. Rafique, S.K. Kailasa, T.J. Park, Recent advances of upconversion nanoparticles in theranostics and bioimaging applications, TrAC Trends Anal. Chem 120 (2019) 115646.
[20] S. Ghosh, S. Jana, D. Nath, N. Guchhait, Fluorescent probing of protein bovine serum albumin stability and denaturation using polarity sensitive spectral response of a charge transfer probe, J. Fluoresc. 21 (2011) 365–374.
[21] S. Jana, S. Dalapati, S. Ghosh, N. Guchhait, Binding interaction between plasma protein bovine serum albumin and flexible charge transfer fluorophore: a spectroscopic study in combination with molecular docking and molecular dynamics simulation, J. Photoch. Photobio., A 231 (2012) 19–27.
[22] S. Jana, S. Dalapati, S. Ghosh, N. Guchhait, Potential charge transfer probe induced conformational changes of model plasma protein human serum albumin: spectroscopic, molecular docking, and molecular dynamics simulation study, Biopolymers 97 (2012) 766–777.
[23] S. Jana, S. Dalapati, S. Ghosh, S. Kar, N. Guchhait, Excited State Charge Transfer reaction with dual emission from 5-(4-dimethylamino-phenyl)-penta-2,4-dienenitrile: Spectral measurement and theoretical density functional theory calculation, J. Mol. Struct 998 (2011) 136–143.
[24] J.W. Wang, G.P. Hua, L.H. Li, D.Y. Li, F.F. Wang, J.Z. Wu, Z.Y. Ye, X. Zhou, S.F. Ye, J. Yang, X.J. Zhang, L. Ren, Upconversion nanoparticle and gold nanocage satellite assemblies for sensitive ctDNA detection in serum, Analyst 145 (2020) 5553–5562.
[25] P.Y. Wang, A.C. Wang, M.M. Hassan, Q. Ouyang, H.H. Li, Q.S. Chen, A highly sensitive upconversion nanoparticles-WS2 nanosheet sensing platform for Escherichia coli detection, Sens. Actuator B-Chem. 320 (2020) 7.
[26] M.K. Tsang, Y.T. Wong, T.H. Tsoi, W.T. Wong, J.H. Hao, Upconversion luminescence sandwich assay for detection of influenza H7 subtype, Adv. Healthc. Mater. 8 (2019) 8.
[27] S. Wu, N. Duan, Z. Shi, C. Fang, Z. Wang, Simultaneous aptasensor for multiplex pathogenic bacteria detection based on multicolor upconversion nanoparticles labels, Anal. Chem. 86 (2014) 3100–3107.
[28] F. Wang, R.R. Deng, X.G. Liu, Preparation of core-shell NaGdF4 nanoparticles doped with luminescent lanthanide ions to be used as upconversion-based probes, Nat. Protoc. 9 (2014) 1634–1644.
[29] J. Lv, S. Zhao, S. Wu, Z. Wang, Upconversion nanoparticles grafted molybdenum disulfide nanosheets platform for microcystin-LR sensing, Biosens. Bioelectron. 90 (2017) 203–209.
[30] L.C. He, Q.Q. Ni, J. Mu, W.P. Fan, L. Liu, Z.T. Wang, L. Li, W. Tang, Y.J. Liu, Y.Y. Cheng, L.G. Tang, Z. Yang, Y. Liu, J.H. Zou, W.J. Yang, O. Jacobson, F. Zhang, P.T. Huang, X.Y. Chen, Solvent-assisted self-assembly of a metal-organic framework based biocatalyst for cascade reaction driven photodynamic therapy, J. Am. Chem. Soc. 142 (2020) 6822–6832.
[31] F. Wang, Y. Han, C.S. Lim, Y. Lu, J. Wang, J. Xu, H. Chen, C. Zhang, M. Hong, X. Liu, Simultaneous phase and size control of upconversion nanocrystals through lanthanide doping, Nature 463 (2010) 1061–1065.
[32] J.X. Zhao, X. Chen, B. Chen, X. Luo, T.Y. Sun, W.W. Zhang, C.J. Wang, J. Lin, D. Su, S. Qiao, F. Wang, Accurate control of core-shell upconversion nanoparticles through anisotropic strain engineering, Adv. Funct. Mater. 29 (2019) 7.
[33] Y. Rong, H. Li, Q. Ouyang, S. Ali, Q. Chen, Rapid and sensitive detection of diazinon in food based on the FRET between rare-earth doped upconversion nanoparticles and graphene oxide, Spectrochim Acta Part A Mol. Biomol. Spectrosc 239 (2020) 118500.
[34] J. Hu, L. Wang, F. Li, Y.L. Han, M. Lin, T.J. Lu, F. Xu, Oligonucleotide-linked gold nanoparticle aggregates for enhanced sensitivity in lateral flow assays, Lab on A Chip 13 (2013) 4352–4357.
[35] W. Hu, Q. Chen, H. Li, Q. Ouyang, J. Zhao, Fabricating a novel label-free aptasensor for acetamiprid by fluorescence resonance energy transfer between NH_2-$NaYF_4$: Yb, Ho@SiO_2 and Au nanoparticles, Biosens. Bioelectron 80 (2016) 398–404.
[36] U.P. Raghavendra, M. Basanagouda, J. Thipperudrappa, Investigation of role of silver nanoparticles on spectroscopic properties of biologically active coumarin dyes 4PTMBC and 1IPMBC, Spectrochim Acta Part A Mol. Biomol. Spectrosc 150 (2015) 350–359.